HHS Public Access

Author manuscript

Methods Mol Biol. Author manuscript; available in PMC 2015 November 10.

Published in final edited form as:

Methods Mol Biol. 2010 ; 606: 247–269. doi:10.1007/978-1-60761-447-0_18.

Studying lipid organization in biological membranes using liposomes and EPR spin labeling

Witold K. Subczynski, PhD, DSc[1,*], **Marija Raguz, MSc**[1], and **Justyna Widomska, PhD**[2]

[1]Department of Biophysics, Medical College of Wisconsin, Milwaukee, WI 53226, USA

[2]Department of Plant Physiology and Biochemistry, Faculty of Biochemistry, Biophysics and Biotechnology, Jagiellonian University, Krakow, Poland

Summary

Electron paramagnetic resonance (EPR) spin-labeling methods provide a unique opportunity to determine the lateral organization of lipid bilayer membranes by discrimination of coexisting membrane domains or coexisting membrane phases. In some cases, the coexisting membrane domains can be characterized by profiles of alkyl chain order, fluidity, hydrophobicity, and oxygen diffusion-concentration product *in situ*, without the need for their physical separation. This chapter briefly explains how the EPR spin-labeling methods can be used to obtain the above mentioned profiles across the lipid bilayer membranes (liposomes) derived from the lipid extract of certain biological membranes. These procedures will be illustrated by EPR measurements performed for multilamellar liposomes made of the lipid extracts from cortical and nuclear fractions of the fiber cell plasma membranes of a cow eye lens. To elucidate better the major factors that determine membrane properties, the results for eye lens lipid membranes will be compared with those obtained for simple model membranes resembling basic lipid composition of biological membranes.

Keywords

Liposomes; lipid bilayer; membrane domain; cholesterol; lens lipid; hydrophobic barrier; fluidity; order; oxygen permeation; spin label; EPR

1. Introduction

Since membranes, and thus membrane domains, are not really two-dimensional structures, the knowledge of the molecular events in the depth dimension is important. The electron paramagnetic resonance (EPR) spin-labeling methods provide this information. Using lipid spin labels with the EPR monitoring groups (free radical nitroxide moieties) located at different depths in the membrane profiles of different membrane properties across the lipid bilayer can be obtained. Because of the overall similarity of the molecular structures of these spin labels with phospholipids and cholesterol (Fig. 1) they should, to a certain degree,

[*]Corresponding Author: Witold K. Subczynski, Department of Biophysics, Medical College of Wisconsin, 8701 Watertown Plank Road, Milwaukee, WI 53226, USA. Tel: (414) 456 4038; Fax: (414) 456 6512; subczyn@mcw.edu.

approximate the distribution of phospholipid and cholesterol molecules between membrane domains, as well as cholesterol-phospholipid and cholesterol-cholesterol interactions in the membrane. These spin labels can be distributed between different membrane domains or membrane phases, what gives possibility not only to discriminate these domains and phases, but also characterize them by profiles of certain membrane properties obtained in coexisting domains and phases without the need for their physical separation. This is the case for the raft domain coexisting within the bulk lipids (1,2,3) or for the liquid-ordered phase coexisting with the liquid-disordered or solid-ordered phases (4,5). This information for coexisting membrane domains is practically missing in the membrane research. For some membrane compositions and membrane lateral organization the distribution of lipid spin label is unique, what allowed obtaining additional information about the structure and dynamics of these coexisting membrane domains. This is the case for membranes overloaded with cholesterol in which pure cholesterol crystalline domains are formed (6). Figure 2 is a schematic drawing illustrating the cases mentioned above. Both, phospholipid type spin labels and cholesterol analogue spin labels are distributed between raft and bulk domain (Fig. 2A) what allowed discrimination of these domains using the discrimination by oxygen transport (DOT) method and obtaining profiles of the oxygen transport parameter (oxygen diffusion-concentration product) across each domain (7). In membranes with the cholesterol crystalline domain, the phospholipid-type spin labels should partition only into the bulk phospholipid-cholesterol domain (Fig. 2B). Thus, additionally to the profile of the oxygen transport parameter, profiles of the order parameter, fluidity, and hydrophobicity can be obtained with the use of these spin labels, which should describe only properties of the bulk phospholipid-cholesterol domain, without “contamination” from the cholesterol crystalline domain (6). The cholesterol analogues should distribute between both domains (Fig. 2B). Thus, only ASL and CSL can detect and discriminate both coexisting domains and allow information about pure cholesterol crystalline domain to be obtained (6).

The DOT method has been already described in the *Methods in Molecular Biology* (7). This method has been successfully applied to discriminate domains in reconstituted membranes crowded with integral membrane proteins (8) as well as in the influenza virus envelope membranes, which contains cholesterol-rich and protein-rich raft domains (1). In model membranes made from binary mixtures of phosphatidylcholine and cholesterol or sphingomyelin and cholesterol, liquid-ordered, liquid-disordered and solid-ordered phases were distinguished and characterized in different regions of a phase diagram when they form a single phase or when two phases coexist (4,5). In membranes made from the ternary raft-forming mixture, the raft domain was also distinguished from bulk lipids with the use of the DOT method (2,3). Similarly, the DOT method can be applied to study the lipid organization in lipid bilayer membranes (liposomes) derived from the lipid extract of certain biological membranes. The main focus of this chapter will be on a new applications of the EPR spin labeling methods to study membranes overloaded with cholesterol, like those of eye lens fiber cell plasma membranes (6,9,10). The presence of the pure cholesterol crystalline domain in these membranes broadened possibilities of the DOT method, which, in combination with the conventional EPR spin-labeling approaches enable one to obtain rather complete information about membrane structure and its physical properties (6).

1.1. EPR spin-labeling approaches for profiles of membrane properties

To obtain detailed profiles across lipid bilayers, a variety of lipid spin labels are incorporated in the membrane for probing at specific depths and specific membrane domains (Fig. 1). EPR spin-labeling methods apply conventional EPR and saturation-recovery EPR techniques. Information obtained from the conventional EPR spectra includes profiles of the order parameter (11) and hydrophobicity (12). Saturation-recovery EPR signals inform primarily about collisions between paramagnetic molecules including nitroxide-nitroxide (13), nitroxide-oxygen (14,15), and nitroxide-paramagnetic metal ions (12), although, these collisions can be extracted from the conventional EPR measurements using line-broadening approach (16) or continuous wave power saturation measurements (17) but without details and with lower precision. Profiles of the spin-lattice relaxation time, obtained directly from the saturaturation-recovery EPR signals, contain also useful information about dynamics (fluidity) of the membrane interior. All presented profiles were obtained for liquid-crystalline phase membranes, except hydrophobicity profiles. Hydrophobicity profiles were drawn based on measurements performed for a frozen suspension of membranes (liposomes) at −150 to −165°C. This is necessary to distinguish between the motional and solvent effects on the EPR spectra (12).

1.2. Detailed profiles across lipid bilayers

To draw a correct profile across the lipid bilayer the knowledge of the position (depths) at which the nitroxide moiety is located in the membrane is very important. However, the existence of vertical fluctuations of the nitroxide moiety of stearic acid spin labels (*n*-SASL) and phospholipid spin labels (*n*-PC) toward the polar surface of the lipid bilayer was reported (13,18). From these studies it can be presumed that distribution of the vertical positions of the nitroxide moiety of *n*-SASL and *n*-PC in the membrane exist, with the mean value of each distribution shifting toward the center as the quantum *n* increases. Positions of carbon atoms in the alkyl chain have been determined by neutron diffraction (19), which showed that the mean positions of these carbons (or nitroxide moieties attached to those carbons) can be defined with accuracy ±1 Å, even in the liquid-crystalline state. Assuming a Gaussian distribution of the labeled segments in the projection on the bilayer normal, these authors reported that the time-averaged positional fluctuations increase from 1.5 Å for the C4 position to 3.4 Å for the C12 position. It can be concluded that a nitroxide moiety stays at the position determined by neutron diffraction for most of the time (*see* Note 1).

1.3. Necessity of measurements for simple membrane models

It is strongly recommended to compare results obtained for membranes made of the lipids extracted from biological membranes with those obtained for simple two-, three-component membranes, made of commercially available lipids, that reflect (resemble) basic lipid composition of biological membranes. This comparison gives a possibility to elucidate better the major factors (to indicate the major membrane components) that determine certain

[1]The thickness of the lens lipid membrane is assumed to be the same as the thickness of the POPC/Chol = 1/1 membrane. It is also assumed that the location of the alkyl chain carbon atom in the membrane change linearly with the position on the alkyl chain. Nitroxide moieties in n-PC and n-SASL are located at the same depth as appropriate carbon atoms of the 2-chain of phospholipid. For details see (15,10,26).

membrane properties. In the presented example of cow eye lens lipid membranes the simple models are membranes made of an equimolar binary mixture of POPC and cholesterol and of pure POPC (9,10). This comparison allowed to conclude that the high cholesterol content in the lipid extracts from the fiber cell plasma membranes is responsible for the unique membrane properties monitored with the use of the EPR spin labeling methods (*see* **Subheading 3.6**).

2. Materials

1. Phospholipid spin labels (1-palmitoyl-2-(n-doxylstearoyl)phosphatidylcholine (n-PC, where n = 5, 7, 10, 12, 14, or 16), or tempocholine-1-palmitoyl-2-oleoylphosphatidic acid ester (T-PC)) can be purchased from Avanti Polar Lipids, Inc. (Alabaster, AL). n-doxylstearic acid spin labels (n-SASL, where n = 5, 7, 9, 10, 12, or 16), cholestane spin label (CSL) and androstane spin label (ASL) can be purchased from Sigma (St. Louis, MO). Spin labels are dissolved in chloroform at 1 mM and stored in a freezer at −70°C.
2. Chloroform solutions of the total lipids extracted from a biological material (usually 5 – 20 mg/mL) are kept in a freezer at −70°C (*see* Note 2).
3. Stock solutions of commercially available lipids (phospholipids and cholesterol) from Avanti Polar Lipids, Inc. (Alabaster, AL) in chloroform (usually 20 – 50 mg/mL) are kept in a freezer at −70°C. These lipids are used to form a simple two-three-component membrane models (see **Subheading 1.3**).
4. Buffers: Typically, 10 mM PIPES and 150 mM NaCl, pH 7.0 is used as a buffer. For samples with n-SASL, 0.1 M borate at pH 9.5 is used as a buffer. In this case a rather high pH is chosen to ensure that all SASL probe carboxyl groups are ionized in lipid bilayer membranes (20,21) (*see* Note 3).

3. Methods

3.1. Spin Labeling

1. Chloroform solutions of extracted lipids and an appropriate spin label are mixed to attain the final concentration of 0.5 or 1 mol% of spin labels in the lipid bilayer (*see* Note 4).
2. Spin labels that allow hydrophobicity profiles and profiles of the oxygen transport parameter across the lipid bilayer to be obtained are n-PC, T-PC, and n-SASL (*see* Fig. 1 for their structures and approximate localization in the lipid bilayer).

---

[2]The commonly used procedure for extraction of lipids from animal tissues was described by Folch and co-authors in 1957 (27). This procedure with minor modification was also used for lipid extraction from cow eye lenses (9,10). The choice of extraction procedure should depend on the nature of the tissue matrix and another factor, for example specific lipid classes. The principles and good practice of tissue handling and lipid separation has been described in many specialist articles, books, and reviews (28,29,30).

[3]At pH 7.0 the mixture of two forms of SASLs can be presented in the lipid bilayer (with protonated and ionized carboxyl groups) and nitroxide moieties of these spin labels can be positioned at two different depths in the membrane.

[4]Too high concentration of spin labels in the lipid bilayer affects measured spectral parameters, especially a spin lattice relaxation time. If the composition of the lipid extract (*see* Note 2) is known, the concentration of spin labels can be easily calculated. Otherwise, the average molecular weight of phospholipids in the total lipid extract has to be assumed and used for the calculation of spin label concentration as in (9).

3. Spin labels that allow profiles of the alkyl chain order parameter across the lipid bilayer to be obtained are n-PC, and n-SASL.

4. Spin labels that allow discrimination of raft and bulk domains (1,2,3) or liquid-ordered, liquid-disordered and solid-ordered phases (4,5) are n-PC, T-PC, and n-SASL (*see* Fig. 2A).

5. Only the spin-labeled cholesterol analogue, ASL, allows discrimination of the cholesterol crystalline domain from the bulk phospholipid-cholesterol domain (6) (*see* Fig. 2B and Subheading 3.5.4).

3.2. Preparation of Multilamellar Liposomes

The membranes used for EPR measurements are usually multilamellar dispersions of lipids (multilamellar liposomes (*see* Note 5)) prepared in the following way:

1. Chloroform solution of lipids and spin label (usually 2–4 mg of total lipid per sample) (*see* **Subheading 3.1 p. 1**) is placed in the glass test tube and chloroform is evaporated with a stream of nitrogen. The lipid film on the bottom of the test tube is thoroughly dried under reduced pressure (about 0.1 mmHg) for about 12 h.

2. A buffer solution (usually 0.5 – 1.0 mL) is added to the dried film at a temperature above the phase transition temperature of investigated membranes (for lipids extracted from biological materials 40°C is sufficient) and vortexed vigorously.

3. The lipid dispersion is centrifuged briefly (15 min at 4°C with an Eppendorf bench centrifuge at 16,000g) and the loose pellet (about 20% lipid, w/w) is used for the EPR measurements.

3.3. Conventional EPR

1 For all EPR measurements the loose pellet is transferred to a capillary made of gas-permeable methyl-pentene polymer known as TPX (*see* Note 6) and the end of capillary is sealed with Baxter Miniseal wax B4425.1 (*see* Notes 7 and [8]). This plastic is permeable to oxygen, nitrogen, and other gases and is substantially impermeable to water.

2 The TPX capillary is fixed inside the EPR dewar insert in the resonator of the X-band EPR spectrometer with a special Teflon holder (*see* Notes 9) and equilibrated with nitrogen gas that is used for temperature control.

3 The sample is thoroughly deoxygenated, yielding correct EPR line shape (*see* Note 10).

---

[5]Membranes in samples made from multilamellar liposomes are tightly packed giving much better signal-to-noise ration than in samples made from unilamellar liposomes

[6]For measurements at X-band these sample tubes are machined from TPX with dimensions of 0.6 mm ID, 0.1 mm wall thickness, and 25 mm length. TPX rods from which the capillaries are machined can be purchased from Midland Plastic (Madison, WI).

[7]This sealant is no longer commercially available, but can be found in many laboratories. Other tube sealant can be used including Critoseal (Fisher Scientific) and X-Sealant (Bruker Biospin).

[8]It is often desirable to additionally concentrate the sample inside the TPX capillary by centrifugation in order to improve the signal-to-noise ratio (31).

[9]TPX capillaries together with the Teflon holder can be obtained from Molecular Specialties (Milwaukee, WI).

4 To obtain profiles of the order parameter the EPR spectra are recorded for spin labels with the nitroxide moiety at different depths in the membrane (*see* **Subheading 3.1 p. 3**). Only one type of spin label molecule is present in each sample. The recording conditions are: the modulation amplitude of 0.5–1.0 G and an incident microwave power about 5 mW.

5 The order parameter, *S*, is calculated using the equation (22)

$$S=0.5407(A'_{\mathrm{II}}-A'_{\perp})/a_0, \quad \text{where} \quad a_0=(A'_{\mathrm{II}}+2A'_{\perp})/3 \quad (1)$$

The values used for the calculation of the hydrocarbon chain order parameter, A'_{II} and $A'_{\perp}$, are measured directly from the EPR spectra as indicated in Fig. 3.

5 To obtain the hydrophobicity profiles across the membrane, the z-component of the hyperfine interaction tensor, A_Z, for spin labels with the nitroxide moiety at different depths in the membrane is determined directly from the EPR spectra for samples frozen at about −165°C as indicated in Fig. 4 (*see* **Subheading 3.1 p. 2**). Only one type of spin label molecule is present in each sample. The recording conditions are: modulation amplitude of 2 G and an incident microwave power of 2 mW (12). In hydrophobicity profiles the A_Z is plotted as a function of the approximate position of the nitroxide moiety in the lipid bilayer (*see* Notes 11).

3.4. Saturation-Recovery EPR (*see* Note 12)

The saturation-recovery EPR method of measuring electron spin-lattice relaxation time (T_1) is a technique in which recovery of the EPR signal is measured at a low level microwave field (weak observing microwave power) after the end of the saturating microwave pulse. The time scale of this recovery is characterized by the spin-lattice relaxation time, T_1.

1 The sample prepared as described in **Subheading 3.2** is transferred to the TPX capillary, positioned in the loop-gap resonator of the saturation-recovery EPR spectrometer and deoxygenated by blowing the nitrogen gas around the TPX capillary (*see* Notes 8 and [10]). Thorough deoxygenation allows measurements correct spin-lattice relaxation time, T_1. The saturation-recovery signal is

[10]Molecular oxygen is paramagnetic, having a triplet ground state, and bimolecular collisions of molecular oxygen with spin labels affect EPR spectral parameters of spin labels including line width and spin-lattice relaxation time (32).

[11]Hydrophobicity profiles are constructed based on the EPR measurements of $2A_Z$ for n-PC and n-SASL spin labels. $2A_Z$ for SASLs in the aqueous phase was calculated as described in (12). In addition T-PC is used to probe the membrane polar headgroup region. Because the chemical structure of the nitroxide moiety of T-PC differs from that for n-PC and n-SASL the $2A_Z$ values measured with T-PC cannot be directly compared with those for n-PC and n-SASL. T-PC reports, however, relative hydrophobicity changes in polar headgroup regions after addition of certain membrane modifiers (like cholesterol). The $2A_Z$ values measured with T-PC can be also used to compare hydrophobicity of polar headgroup regions in different membranes.

[12]The home-built state-of-the-art X-band and Q-band saturation-recovery EPR spectrometers are available at the National Biomedical EPR Center, Medical College of Wisconsin, Milwaukee, WI, USA. The mission of the Center is to make advanced EPR Research Resources available to investigators nationally, regionally and locally (see the link for Center use: http://www.mcw.edu/display/router.asp?docid=3211). Another home-built X-band saturation-recovery spectrometer is located at the Department of Biophysics, Faculty of Biotechnology, Jagiellonian University, Krakow, Poland. Presently Bruker produces EPR spectrometers capable for saturation-recovery measurements at X-band. Doing pulse saturation recovery is possible on an E-580 FT/EPR system equipped with the DC-AFC and LCW (low power CW arm) options combined with the AmpX CW microwave power amplifier. Saturation recovery is treated as an accessory to the E-580 and is not usually a stand-alone configuration.

recorded at the required temperature for the spin label with the nitroxide moiety at a fixed depth in the membrane. Only one type of spin label molecule is present in each sample.

3 To get values of the oxygen transport parameter the saturation-recovery signal is also recorded for the same sample equilibrated with the required partial pressure of oxygen at the required temperature (*see* Note 13).

4 The same procedure is repeated for other spin labels with the nitroxide moieties at different depths in the membrane (*see* **Subheading 3.1 p. 2**). 5. The T_1s of spin labels in the absence and presence of molecular oxygen are determined by analyzing the saturation-recovery signal of the central line obtained by short-pulse saturation-recovery EPR (*see* Note 14).

6 The pulse length for short-pulse experiments is in the range of 0.1 – 0.5 μs. Pump power is selected to maximize the amplitude of the saturation-recovery signal and is typically in the range of 2 – 3.5 G. Observing power is selected to be as high as possible without affecting the time constant of the recovery. The minimum time between the end of the pulse and the beginning of observation of the recovery is determined by the ring-down time of the resonator and the switching transients and is usually longer than 0.35 μs. Typically 10^5 – 10^6 decays are acquired with 2048 data points on each decay. Sampling intervals are from 1 to 32 ns depending on sample, temperature and oxygen tension. The total accumulation time is typically 2 – 5 min.

7 Saturation-recovery signals are fitted by single and double exponentials and compared (*see* Fig. 5). If no substantial improvement in the fitting is observed when the number of exponentials is increased from one, the recovery curves can be analyzed as single exponential (*see* Fig. 5A,B,C,D,E) (*see* Note 15). This is often the case for samples equilibrated with nitrogen (Fig. 5A,C,E). For samples equilibrated with different partial pressure of oxygen, the saturation-recovery signal often can be fitted successfully only with the double-exponential curve (as shown in Fig. 5F) indicating the presence of two coexisting domains or two coexisting phases (*see* Note 16).

8 Calculation of the oxygen transport parameter from single exponential decays (*see* Fig. 5A,B,C,D,E)

---

[13]Switching the gas around the TPX capillary from nitrogen to the air/nitrogen mixture allows one to easily equilibrate the sample with the required partial pressure of oxygen for oximetry measurements and for obtaining T_1s in the presence of molecular oxygen. Because the same gas mixture is used for temperature control, samples are equilibrated with oxygen at the required temperature. The mixture of air and nitrogen is adjusted with flowmeters ((Matheson Gas Products, Montgomeryville, PA, model 7631 H-604).

[14]The short-pulse method is favorable for multiexponential decays in oximetry measurements (33,34). For a short pulse, only populations of the irradiated transition are affected; for a long pulse, all populations are altered because of transverse relaxations. Ref. (35) addresses the long- and short-pulse saturation-recovery methods in more detail.

[15]Additional criteria for the goodness of a single exponential fit are the negligible preexponential coefficient for the second component, the large standard deviation of T_1 for the second component, and the repetition of the fit for different recording conditions such as number of points and time increment.

[16]Although, the saturation-recovery signals in the absence of molecular oxygen cannot differentiate between these two domains, in the presence of oxygen the recovery curves are very different in each domain, indicating that the collision rate of molecular oxygen, or the oxygen transport parameter, is quite different in these two domains. This is a good illustration of why the method is named DOT, because different domains can be clearly discriminated and characterized only in the presence of molecular oxygen.

The oxygen transport parameter is calculated using the equation (14)

$$W(\mathrm{x}) = T_1^{-1}(\mathrm{Air},\ \mathrm{x}) - T_1^{-1}(\mathrm{N_2},\ \mathrm{x}) = AD(\mathrm{x})C(\mathrm{x}) \quad (2)$$

T_1(Air, x) and T_1(N_2, x) are spin-lattice relaxation times of nitroxides in samples equilibrated with atmospheric air and nitrogen, respectively. Note that W(x) is normalized to the sample equilibrated with the atmospheric air. W(x) is proportional to the product of the local translational diffusion coefficient D(x) and the local concentration C(x) of oxygen at a depth x in the membrane, which is in equilibrium with the atmospheric air (*see* Note 17).

9 Calculation of the oxygen transport parameter from double exponential decays (*see* Fig. 5F).

In membranes consisting of two lipid environments with different oxygen transport rates—the fast oxygen transport (FOT) domain and the slow oxygen transport (SLOT) domain—the saturation-recovery signals recorded for samples equilibrated with air and nitrogen are simple double-exponential curves with time constants of T_1^{-1}(Air, FOT), T_1^{-1}(Air, SLOT) and T_1^{-1}(N_2, FOT), T_1^{-1}(N_2, SLOT), respectively (1,4,5,7,8) (*see* Note 18). Thus, values of the oxygen transport parameter in each domain can be calculated using equations:

$$W(\mathrm{FOT}) = T_1^{-1}(\mathrm{Air},\ \mathrm{FOT}) - T_1^{-1}(\mathrm{N_2},\ \mathrm{FOT}) \quad (3)$$

$$W(\mathrm{SLOT}) = T_1^{-1}(\mathrm{Air},\ \mathrm{SLOT}) - T_1^{-1}(\mathrm{N_2},\ \mathrm{SLOT}) \quad (4)$$

Here "x" from Eq. 2 is changed to the two-membrane domain FOT and SLOT and the depth fixed (the same spin label is distributed between the FOT and SLOT domains).

3.5. Profiles of Membrane Properties Across Homogeneous Membranes and Across Coexisting Membrane Domains

The final goal in the studies of lipid organization in biological membranes using liposomes and EPR spin labeling is not only to characterize them by single (at one depth) spectral parameters, but to obtain detailed profiles of these parameters across membranes. These detailed profiles contain unique information about the membrane structure and dynamics. Additionally, these profiles can often be obtained in coexisting membrane domains without the need for their physical separation, which provides unique opportunities in studies of physical properties of domains *in situ*. Using various spin-labeling techniques as well as conventional and saturation-recovery EPR spectroscopy (covering a time scale of 100 ps – 10 μs) the membrane molecular organization and dynamics can be investigated in the ps-to-μs regime. Below, profiles of four parameters obtained with EPR spin-labeling methods and

[17] A is remarkably independent of the hydrophobicity and viscosity of the solvent and of spin label species (36,37,38).

[18] When located in two different membrane domains, the spin label alone most often cannot differentiate between these domains, giving very similar conventional EPR spectra and similar T_1 values (T_1^{-1}(N_2, FOT) T_1^{-1}(N_2, SLOT)). However, even small differences in lipid packing in these domains will affect oxygen partitioning and oxygen diffusion, which can be easily detected by observing the different T_1s from spin labels in these two locations in the presence of oxygen.

describing different properties of biological and model membranes are presented with a short explanation about the information which can be extracted from those profiles.

3.5.1. Order Parameter—In the membrane, the alkyl chain of *n*-PC or *n*-SASL with the nitroxide moiety attached at the C*n* position (*see* Fig. 1) undergoes rapid anisotropic motion about the long axis of the spin label and wobbling motion of the long axis within the confines of a cone imposed by the membrane environment. Order parameter (Eq. 1) is a measure of the amplitude of the wobbling motion. Increase in an order parameter indicates that the cone angle of the cone for the wobbling motion of the alkyl chain decrease. Moreover, deviations in the alkyl chain segment direction from the bilayer normal accumulate as one proceeds from the bilayer surface to the membrane interior, a result of the effective tethering of the alkyl chain at the bilayer surface. Consequently, ordering of the alkyl chain induced by the steric contact with the plate-like portion of cholesterol will also cause ordering of the distal fragment of the alkyl chain, even though the rate of wobbling fluctuations can be higher (9,13) (*see* **Subheading 3.5.2**). Although, the order parameter indicates the static property of the lipid bilayer, for brevity, the change in the order parameter is most often described as the change of spin label mobility, and thus, as the change of membrane fluidity.

Profiles of the molecular order parameter obtained at 25°C for the bulk phospholipid-cholesterol domain of cortical and nuclear cow lens lipid membranes are displayed in Fig. 6A. In both membranes values of the order parameter measured at the same depths are practically the same and are close to those measured for membranes made of the equimolar POPC/cholesterol mixture (Fig. 6B). They are, however, significantly greater than those measured for the pure POPC membrane (Fig. 6B), indicating, that saturating amount of cholesterol is responsible for lens membrane rigidity. In all membranes profiles have an inverted-bell-shape and the alkyl chain order gradually decreases with an increase of the depth in the membrane.

3.5.2. Fluidity—There are no easy obtainable EPR spectral parameters for lipid spin labels that can describe profiles of the membrane fluidity related to the dynamic membrane properties. Only in the membrane center membrane fluidity can be evaluated directly from the conventional EPR spectra of 16-PC (or 16-SASL) by measuring the effective rotational correlation time of the nitroxide moiety of this lipid spin label, assuming its isotropic rotational motion (23). This assumption is already not fulfilled for 14-PC which shows anisotropic rotational motion. Also, in the presence of 30 mol% cholesterol, motion of 16-PC is going to the slow tumbling regime, where no conventional parameterization has been established (*see* Note 19). As was indicated in the **Subheading 3.5.1**, the order parameter, which is most often used as a measure of membrane fluidity, describes, in principle, the static membrane properties, namely the amplitude of the wobbling motion. Fortunately, the spin lattice relaxation time (T_1) is a spectral parameter which can be easily obtained from the

[19]In principle, the rotational motion of 16-PC molecule as a whole, which is anisotropic, has to be distinguished from segmental motion, which comes from gauche-trans isomerisation of the alkyl chain. For carbon atoms near the terminal methyl group (16-PC position), it is assumed that the segmental motion is not restricted, and as a result, motion of the nitroxide moiety is approximately isotropic. At higher temperatures, the motion of all molecules becomes so great that segmental motion dominates. At lower temperatures, the segmental motion is diminished and the motion of 16-PC become more highly anisotropic.

saturation-recovery EPR measurements with lipid spin labels (see **Subheading 3.4**). This parameter depends primarily on the rate of motion of the nitroxide moiety within the lipid bilayer, and thus describes the dynamics of membrane environment at the depth at which the nitroxide fragment is located. It should be mentioned here that both, the rotational motion (24) and the Brownian translational motion (25) are motional mechanisms involved in the spin lattice relaxation process of nitroxide spin labels. Thus, T_1 can be used as a conventional quantitative measure of membrane fluidity that reports on the rate of motion of phospholipid alkyl chains (or nitroxide free radical moieties attached to those chains).

If the T_1 is measured for *n*-PC or *n*-SASL spin labels, the fluidity profile across the lipid bilayer can be obtained that reflects membrane dynamics. In principle, these fluidity profiles can be obtained in coexisting domains and coexisting phases without the need for their physical separation (see Note 18). These fluidity profiles (T_1 versus depth in the membrane) for the bulk phospholipid-cholesterol domain of the cortical and nuclear cow lens lipid membranes obtained at 25°C are presented in Fig. 7A. As expected, membrane fluidity (membrane dynamics) increases towards the membrane center and profiles in both membranes are inverted-bell-shaped. They are similar to profiles obtained for the membranes made of the equimolar POPC/cholesterol mixture and pure POPC (Fig. 7B). As can be seen from the comparison of the profile for pure POPC bilayer with the profile for POPC/cholesterol bilayer (Fig. 7B) cholesterol decreases membrane fluidity close to the membrane surface and increases it at the membrane center. This confirms reported earlier (13,15,26) (*see* Note 20). The order parameter (the static membrane property) cannot differentiate the effects of cholesterol at different depths (*see* **Subheading 3.5.1**), while another dynamic parameter, namely the oxygen transport parameter clearly shows these differences between the membrane region where cholesterol ring structure is located and the dipper region where the isooctyl chain of cholesterol is located (*see* **Subheading 3.5.4**).

3.5.3. Hydrophobicity—Figure 8A shows hydrophobicity profiles across the bulk phospholipid-cholesterol domain of cortical and nuclear cow lens lipid membranes. Here, the $2A_Z$ data, obtained as described in **Subheading 3.3. p. 5**, are presented as a function of the approximate position of the nitroxide moiety of the spin label within the lipid bilayer. Smaller $2A_Z$ values (upward changes in the profiles) indicate higher hydrophobicity. In both membranes the hydrophobicity profiles show similar rectangular shape, with an abrupt increase of hydrophobicity between the C9 and C10 positions. The $2A_Z$ values in the center of both membranes (positions of 10-, 12-, 14-, and 16-PC) indicate that hydrophobicity in this region is only slightly lower than that for pure hexane ($\varepsilon = 2$) and can be compared to that of ??? (*see* Note 21).

[20]To the best of our knowledge the profile of the spin-lattice relaxation time is used here for the first time as a monitor of membrane dynamics and membrane fluidity. It should be indicated that T_1 is sensitive to the molar concentration of spin labels in the lipid bilayer. Because of that the concentration of all spin labels in the lipid bilayer should be the same, as well as in membranes that are compared. This is not an easy task, especially for the lipid bilayer membranes (liposomes) derived from the lipid extract of certain biological membranes. This is probably the reason why profiles for cortical and nuclear lens lipid membranes presented in Fig 7A are shifted relatively to each other. Other EPR spectral parameters (molecular order, hydrophobicity, oxygen transport parameter) are affected by spin label concentration much less. The profile for POPC presented in Fig. 7B was based on the data obtained in 2003 (40) and that for POPC/Chol was based on the data obtained in 2007 (9). The effects of cholesterol on T_1 of the lipid spin labels located in the membrane center and close to the membrane surface were also clearly shown in (13,15,26).

It is seen from Fig. 8A that the center of the bulk phospholipid-cholesterol domain of the nuclear membrane is less hydrophobic than that of the cortical membrane. Similar difference is also observed close to the membrane surface (5- and 7-PC positions). These interesting findings are in good agreement with an earlier observation (12) that the cholesterol causes the significant increase of the hydrophobicity of the PC lipid bilayer center when its concentration increases up to ~30 mol%, which is followed by the moderate decrease of hydrophobicity when cholesterol concentration increase further, up to 50 mol%. Addition of cholesterol (from 0 to 50 mol%) monotonically decreases hydrophobicity in the region close to the membrane surface. It confirms that the cortical bulk phospholipid-cholesterol domain did not yet reach saturation with cholesterol, while the nuclear bulk phospholipid-cholesterol bilayer is saturated with cholesterol.

Profiles presented in Fig. 8A are similar to that measured for the membrane made of the equimolar POPC/cholesterol mixture (Fig. 8B), which shows also rectangular shape and an abrupt increase of hydrophobicity between the C9 and C10 positions, but differ completely from the typical bell-shape profile for the membrane made of pure POPC (Fig. 8B) with a graduate increase of hydrophobicity toward the bilayer center. Also the change in hydrophobicity between membrane surface and membrane center is significantly lower for pure POPC membrane than for cortical and nuclear membranes. It is concluded that the rectangular shape of the hydrophobicity profiles is characteristic for membranes with a high cholesterol content.

3.5.4. Oxygen Transport Parameter—The oxygen transport parameter was introduced as a conventional quantitative measure of the rate of the collision between spin label and molecular oxygen (Eq. 2). Kusumi at al. (14) concluded that the oxygen transport parameter is a useful monitor of membrane fluidity that reports on translational diffusion of small molecules. The profiles of the oxygen transport parameter for the bulk phospholipid-cholesterol domain of the cortical and nuclear cow lens lipid membranes obtained at 25°C are presented in Fig. 9A (*see* Note 22). All profiles have the rectangular shape with an abrupt increase of the oxygen transport parameter between the C9 and C10 positions. This abrupt increase is as large as 2-3 times, and the overall change of the oxygen transport parameter across the membrane becomes as large as ~5 times. The oxygen transport parameter from the membrane surface to the depth of the ninth carbon is as low as in gel-phase PC membranes, and at locations deeper then the ninth carbon, as high as in fluid-phase membranes (4,9,11,15,26). These profiles are practically identical if we take into account the accuracy of the measurements, evaluated as 10%. Profiles are also very similar to that for the membrane made of the equimolar mixture of POPC and cholesterol (Fig. 9B)

[21]For brevity, we relate the local hydrophobicity as observed by $2A_Z$ to the hydrophobicity (or ε) of the bulk organic solvent by referring to Fig. 2 in Ref. (12). $2A_Z$ in the bulk solvent provides a convenient yardstick for describing local hydrophobicity in the membrane, and comparison of two $2A_Z$ values may help to develop “feel” for local hydrophobicity. Such a comparison is only semi quantitative and could be done operationally because small changes in $2A_Z$ correspond to large changes in ε and because the mechanism by which the presence of water affects $2A_Z$ is not well understood (12,39).

[22]Restrictions for the distribution of lipid spin labels in membranes containing cholesterol crystalline domain, indicate that only spin-labeled cholesterol analogues could discriminate this domain (6). These analogues should approximate the distribution of cholesterol molecules in the membrane because of the overall similarity of CSL, ASL, and cholesterol molecular structures. Phospholipid spin labels, which should not partition into the cholesterol crystalline domain, cannot discriminate these domains. Indeed, in both cortical and nuclear membranes, saturation-recovery signals for n-PCs, 9-SASL, and T-PC were single-exponential signals. They were assigned as signals characterizing the bulk phospholipid-cholesterol bilayer.

which also shows the rectangular shape and an abrupt increase of the oxygen transport parameter between the C9 and C10 positions. However, profiles for cortical and nuclear membranes differ from bell-shaped profile across the pure POPC bilayer (Fig. 9B). This additionally confirms that a high cholesterol content is responsible for the unique property of lens lipid membranes. It should be also indicated that the abrupt change in hydrophobicity (Fig. 8) and oxygen transport parameter profiles (Fig. 9) is observed between the C9 and C10 positions, which is approximately where the steroid ring structure of cholesterol reaches into the membrane.

Only in nuclear membranes equilibrated with air/nitrogen mixture ASL shows two-exponential saturation-recovery signals (Fig. 5F), which indicates the presence of two membrane environments around ASL (*see* Eqs. 3 and 4 and Notes 18 and [22]). Comparison values of the oxygen transport parameter obtained with ASL and those obtained with phospholipid-type spin labels in the bulk phospholipid-cholesterol domain allows concluding that the ASL molecules which give a greater oxygen transport parameter are located in the bulk phospholipid-cholesterol domain (see profile of the oxygen transport parameter for the nuclear lens lipid membrane with added points for the cholesterol analogue spin labels in Fig. 9A). The greater oxygen transport parameter value monitored with ASL is practically the same as the value obtained with 10-PC. This confirms that in the bulk phospholipid-cholesterol bilayer the nitroxide moiety of ASL is located close to the C10 position (6). The second value of the oxygen transport parameter monitored by ASL is about 3 times smaller than the value monitored by ASL in the bulk phospholipid-cholesterol domain and can be assigned as that characterizing the pure cholesterol crystalline domain.

In cortical membranes ASL in the presence and absence of oxygen always showed single-exponential saturation-recovery signal indicating homogenous environment detected by this spin label (Fig. 5A). The oxygen transport parameter value detected by ASL was practically the same as that detected by 10-PC. It allowed assuming that cortical membranes consist of the bulk phospholipid-cholesterol domain without a detectable cholesterol crystalline domain. The CSL in both cortical and nuclear membranes detect only homogenous environments showing always single-exponential saturation-recovery signals. Thus, the oxygen transport parameter values detected in polar headgroup region of the nuclear lens lipid membrane with CSL located in the bulk phospholipid-cholesterol domain and in cholesterol crystalline domain are very similar and cannot be distinguished by the DOT method (*see* Note 23). These results are in the principal agreement with those obtained with ASL and CSL in pig lens lipid membranes in which the cholesterol crystalline domain was induced by the addition of excess cholesterol (6). Values of the oxygen transport parameter

[23]Results presented in Fig. 5 and Fig. 9 is an excellent illustration of the advantages and limitations of the DOT method. To detect membrane domains, lipid spin label have to be distributed between these domains (like CSL and ASL but not like n-PC (*see* Fig. 2B)). Even, when located in two different membrane domains, the spin label alone most often cannot differentiate between these domains, giving very similar T_1 values (in the absence of oxygen saturation-recovery signals for both CSL and ASL were single-exponential signals (Fig. 5) indicating, that T_1 values in both environments are very close). In membranes equilibrated with air and consisting of two lipid environments with different oxygen transport rates: fast oxygen transport (FOT) domain and slow oxygen transport (SLOT) domain, the saturation-recovery signal should be a double-exponential curve with time constants of T_1(air, FOT) and T_1(air, SLOT) (see **Subheading 3.5** and Eqs. 3 and 4). This is the case with ASL which shows the double-exponential saturation recovery signals for sample equilibrated with air/nitrogen mixture (Fig. 5F). CSL cannot distinguish these domains (Fig. 5C,D), probably, because collision rates between oxygen and the nitroxide moiety of CSL located in the polar headgroup region are similar in these two domains.

measured with CSL and ASL in the nuclear lens lipid membrane are indicated in Fig 9A and the profile of the oxygen transport parameter across the cholesterol crystalline domain that coexists with the bulk phospholipid-cholesterol domain, is drown.

Acknowledgments

This work was supported by grants EY015526, EB002052 and EB001980 of the NIH.

References

1. Kawasaki K, Yin J-J, Subczynski WK, Hyde JS, Kusumi A. Pulse EPR detection of lipid exchange between protein-rich raft and bulk domains in the membrane: methodology development and its application to studies of influenza viral membrane. Biophys J. 2001; 80:738–748. [PubMed: 11159441]
2. Wisniewska A, Subczynski WK. Accumulation of macular xanthophylls in unsaturated membrane domains. Free Radic Biol Med. 2006; 40:1820–1826. [PubMed: 16678020]
3. Wisniewska A, Subczynski WK. Distribution of macular xanthophylls between domains in a model of photoreceptor outer segment membranes. Free Radic Biol Med. 2006; 41:1257–1265. [PubMed: 17015172]
4. Subczynski WK, Wisniewska A, Hyde JS, Kusumi A. Three-dimensional dynamic structure of the liquid-ordered domain as examined by a pulse-EPR oxygen probing. Biophys J. 2007; 92:1573–1584. [PubMed: 17142270]
5. Wisniewska A, Subczynski WK. The liquid-ordered phase in sphingomyelin-cholesterol membranes as detected by the discrimination by oxygen transport (DOT) method. Cell Mol Biol Lett. 2006 in press. 10.2478/sl1658-008-0012-y
6. Raguz M, Widomska J, Dillon J, Gailard ER, Subczynski WK. Characterization of lipid domains in reconstituted porcine lens membranes using EPR spin-labeling approaches. Biochim, Biophys Acta. 2008; 1778:1079–1090. [PubMed: 18298944]
7. Subczynski, WK.; Widomska, J.; Wisniewska, A.; Kusumi, A. Saturation-recovery electron paramagnetic resonance discrimination by oxygen transport (DOT) method for characterizing membrane domains. In: McIntosh, TJ., editor. Methods in Molecular Biology 398: Lipid Rafts. Humana Press; Totowa: 2007. p. 143-157.
8. Ashikawa I, Yin JJ, Subczynski WK, Kouyama T, Hyde JS, Kusumi A. Molecular organization and dynamics in bacteriorhodopsin-rich reconstituted membranes: discrimination of lipid environments by the oxygen transport parameter using a pulse ESR spin-labeling technique. Biochemistry. 1994; 33:4947–4952. [PubMed: 8161556]
9. Widomska J, Raguz M, Dillon J, Gaillard ER, Subczynski WK. Physical properties of the lipid bilayer membrane made of calf lens lipids: EPR spin labeling studies. Biochim Biophys Acta. 2007; 1768:1454–1465. [PubMed: 17451639]
10. Widomska J, Raguz M, Subczynski WK. Oxygen permeability of the lipid bilayer membrane made of calf lens lipids. Biochim Biophys Acta. 2008; 1768:2636–2645.
11. Subczynski WK, Lewis RNAH, McElhaney RN, Hodges RS, Hyde JS, Kusumi A. Molecular organization and dynamics of 1-palmitoyl-2-oleoylphosphatidylcholine bilayers containing a transmembrane α-helical peptide. Biochemistry. 1998; 37:3156–3164. [PubMed: 9485469]
12. Subczynski WK, Wisniewska A, Yin JJ, Hyde JS, Kusumi A. Hydrophobic barriers of lipid bilayer membranes formed by reduction of water penetration by alkyl chain unsaturation and cholesterol. Biochemistry. 1994; 33:7670–7681. [PubMed: 8011634]
13. Yin J-J, Subczynski WK. Effects of lutein and cholesterol on alkyl chain bending in lipid bilayers: a pulse electron spin resonance spin labeling study. Biophys J. 1996; 71:832–839. [PubMed: 8842221]
14. Kusumi A, Subczynski WK, Hyde JS. Oxygen transport parameter in membranes as deduced by saturation recovery measurements of spin-lattice relaxation times of spin labels. Proc Natl Acad Sci USA. 1982; 79:1854–1858. [PubMed: 6952236]

15. Subczynski WK, Hyde JS, Kusumi A. Oxygen permeability of phosphatidylcholine-cholesterol membranes. Proc Natl Acad Sci USA. 1989; 86:4474–4478. [PubMed: 2543978]
16. Smirnov AI, Clarkson RB, Belford RL. EPR linewidth (T_2 method to measure oxygen permeability of phospholipids blayer and its use to study the effect of low ethanol concentration. J Magn Reson B. 1996; 111:149–157. [PubMed: 8661272]
17. Altenbach C, Froncisz W, Hyde JS, Hubbell WL. Conformation of spin-labeled melittin at membrane surface investigated by pulse saturation recovery and continuous wave power saturation electron paramagnetic resonance. Biophys J. 1989; 56:1183–1191. [PubMed: 2558734]
18. Merkle H, Subczynski WK, Kusumi A. Dynamic fluorescence quenching studies on lipid mobilities in phosphatidylcholine-cholesterol membranes. Biochim Biophys Acta. 1987; 897:238–248. [PubMed: 3028480]
19. Zaccai G, Büldt G, Seelig A, Seelig J. Neutron diffraction studies on phosphatidylcholine model membranes II. Chain conformation and segmental disorder. J Mol Biol. 1979; 134:693–706. [PubMed: 537075]
20. Egreet-Charlier M, Sanson A, Ptak M, Bouloussa O. Ionization of fatty acids at lipid-water interface. FEBS Lett. 1978; 89:313–316. [PubMed: 207576]
21. Kusumi A, Subczynski WK, Hyde JS. Effects of pH on ESR spectra of stearic acid spin labels in membranes: probing the membrane surface. Fed Proc. 1982; 41:1394.
22. Marsh, D. Electron spin resonance: spin labels. In: Grell, E., editor. Membrane Spectroscopy. Springer-Verlag; Berlin: 1981. p. 51-142.
23. Berliner LJ. Spin labeling in enzymology: spin-labeled enzymes and proteins. Rotational correlation times calculation. Methods Enzymol. 1978; 49:466–470.
24. Atkins PW, Kivelson D. ESR linewidth in solution. II. Analysis of spin-rotational relaxation data. J Chem Phys. 1966; 44:169–174.
25. Robinson BH, Hass DA, Mailer C. Molecular dynamics in lipid spin lattice relaxation of nitroxide spin labels. Science. 1994; 263:490–493. [PubMed: 8290958]
26. Subczynski WK, Hyde JS, Kusumi A. Effect of alkyl chain unsaturation and cholesterol intercalation on oxygen transport in membranes: a pulse ESR spin labeling study. Biochemistry. 1991; 30:8578–8590. [PubMed: 1653601]
27. Folch J, Lees M, Sloane Stanley GH. A simple method for the isolation and purification of total lipids from animal tissues. J Biol Chem. 1957; 226:497–509. [PubMed: 13428781]
28. Markham JE, Li J, Cahoon EB, Jaworski JG. Separation and identification of major plant sphingolipid classes from leaves. J Biol Chem. 2006; 281:22684–22694. [PubMed: 16772288]
29. Bodennec J, Pelled D, Futerman AH. Aminopropyl solid phase extraction and 2 D TLC of neutral glycosphingolipids and neutral lysoglycosphingolipids. J Lipid Res. 2003; 44:218–226. [PubMed: 12518041]
30. Christie, WW. Lipid Analysis (3rd Edition); Isolation, separation, identification and structural analysis of lipids. Oily Press; Bridgwater: 2003.
31. Subczynski WK, Felix CC, Klug CS, Hyde JS. Concentration by centrifugation for gas exchange EPR oximetry measurements with loop-gap resonators. J Magn Reson. 2005; 176:244–248. [PubMed: 16040261]
32. Subczynski, WK.; Swartz, HM. EPR oximetry in biological and model samples. In: Eaton, SS.; Eaton, GR.; Berliner, LJ., editors. *Biological Magnetic Resonance*Biomedical EPR – Part A: Free Radicals, Metals, Medicine, and Physiology. Vol. 23. Kluwer/Plenum; New York: 2005. p. 229-282.
33. Yin JJ, Hyde JS. Spin-label saturation-recovery electron spin resonance measurements of oxygen transport in membranes. Z Phys Chem (Munich). 1987; 153:57–65.
34. Hyde JS, Yin J-J, Feix JB, Hubbell WL. Advances in spin label oximetry. Pure Appl Chem. 1990; 62:255–260.
35. Yin J-J, Hyde JS. Use of high observing power in electron spin resonance saturation-recovery experiments in spin-labeled membranes. J Chem Phys. 1989; 91:6029–6035.
36. Hyde JS, Subczynski WK. Simulation of ESR spectra of the oxygen-sensitive spin-label probe CTPO. J Magn Reson. 1984; 56:125–130.

37. Hyde, JS.; Subczynski, WK. Spin-label oximetry. In: Berliner, LJ.; Reuben, J., editors. Biological Magnetic Resonance. Vol. 8. Plenum Press; New York: 1989. p. 399-425.

38. Subczynski WK, Hyde JS. Diffusion of oxygen in water and hydrocarbons using an electron spin resonance spin-label technique. Biophys J. 1984; 45:743–748. [PubMed: 6326877]

39. Griffith OH, Dehlinger PJ, Van SP. Shape of the hydrophobic barrier of phospholipids bilayers (Evidence for water penetration into biological membranes). J Membr Biol. 1974; 15:159–192. [PubMed: 4366085]

40. Subczynski WK, Pasenkiewicz-Gierula M, McElhaney RN, Hyde JS, Kusumi A. Molecular dynamics of 1-palmitoyl-2-oleoylphosphatidylcholine membranes containing transmembrane α-helical peptides with alternating leucine and alanine residues. Biochemistry. 2003; 42:3939–3948. [PubMed: 12667085]

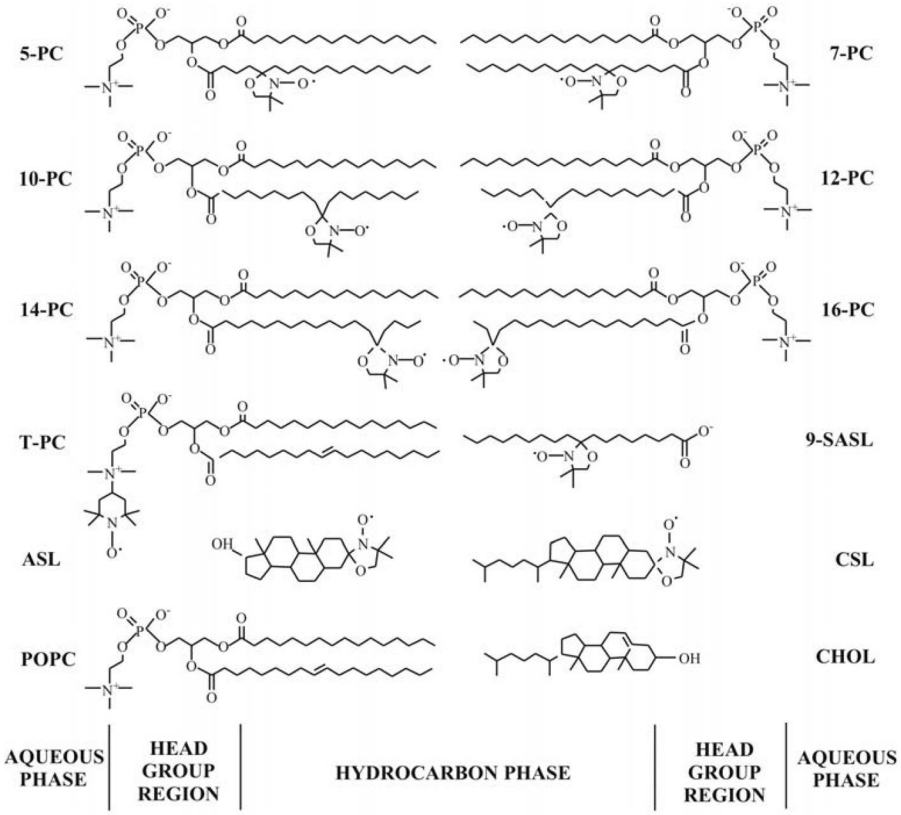

Fig. 1.

Chemical structures of lipid spin labels, phospholipid analog: n-PC, T-PC, and n-SASL, and cholesterol analog: CSL and ASL. Chemical structures of POPC and cholesterol molecules are included to illustrate approximate localizations of these molecules and nitroxide moieties of spin-labels across the membrane.

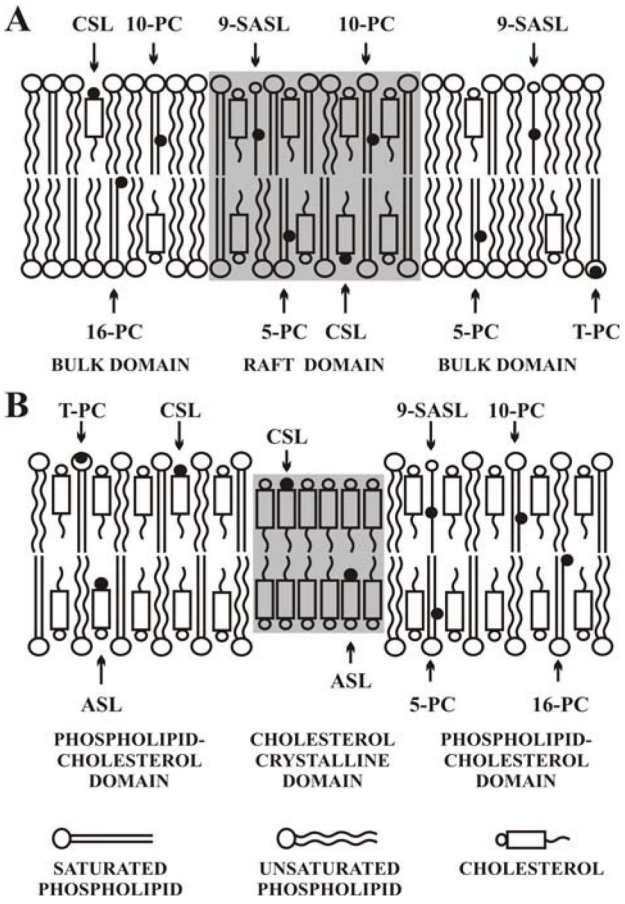

Fig. 2.

Schematic drawing of the raft domain in the bulk lipids (A), and the pure cholesterol-crystalline domain in the bulk phospholipid-cholesterol bilayer (B). The distribution and approximate localization of lipid spin labels in these domains is also shown. Phospholipid spin labels, 5-, 10-, 16-, T-PC and 9-SASL are distributed between the raft domain and bulk lipids (A), and are located only in the bulk phosphopipid-cholesterol domain when this domain coexists with the pure cholesterol crystalline domain (B). Spin-labeled cholesterol analogues, ASL and CSL, are distributed between both domains for coexisting raft domain and bulk lipids (A) and for coexisting cholesterol crystalline domain and bulk phospholipid-cholesterol domain (B). The nitroxide moieties of spin lebels are indicated as black dots.

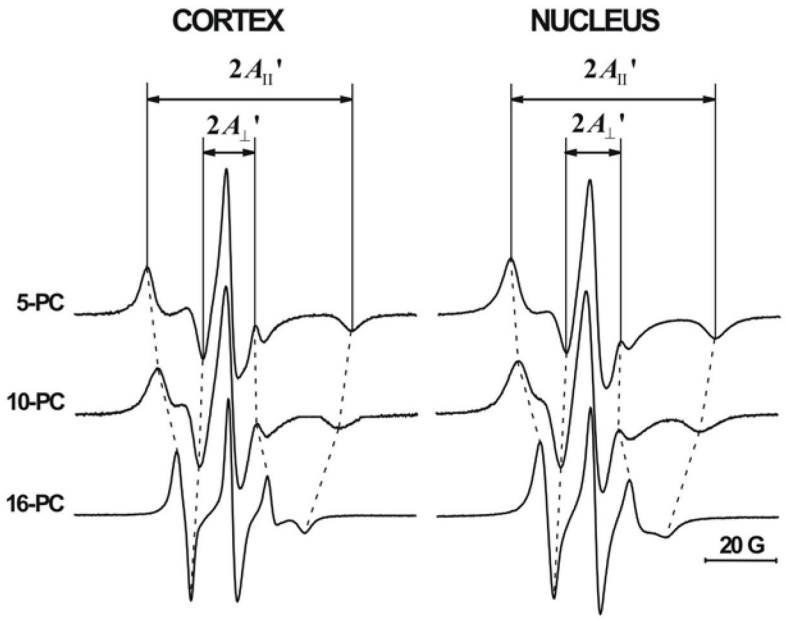

Fig. 3.

Panel of EPR spectra of 5-, 10-, and 16-PC in membranes made of cortical and nuclear cow lens lipids. Spectra were recorded at 25°C. Measured values for evaluating the order parameter are indicated. The positions of certain peaks were evaluated with a high level of accuracy by monitoring them at 10 times higher receiver gain and, when necessary, at higher modulation amplitude.

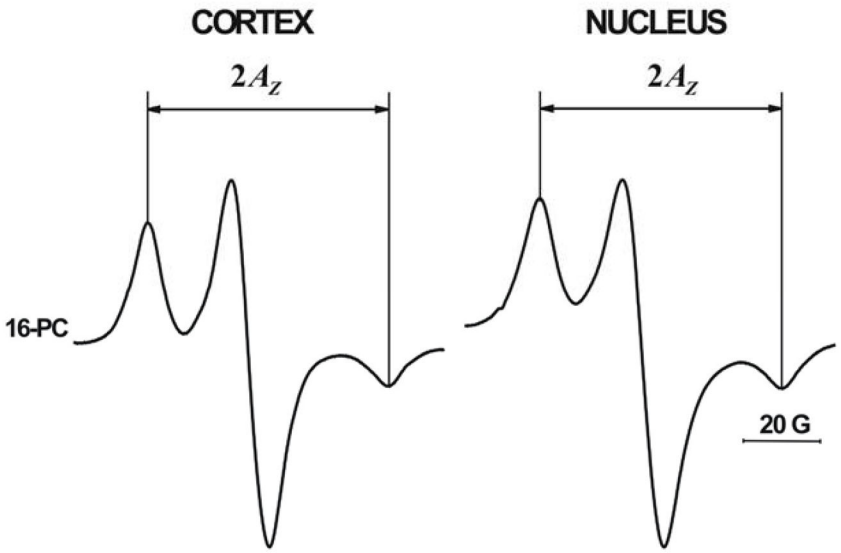

Fig. 4.

EPR spectra of 16-PC in membranes made of cortical and nuclear cow lens lipids. Spectra were recorded at − 163°C to cancel motional effects. The measured $2A_Z$ value is indicated.

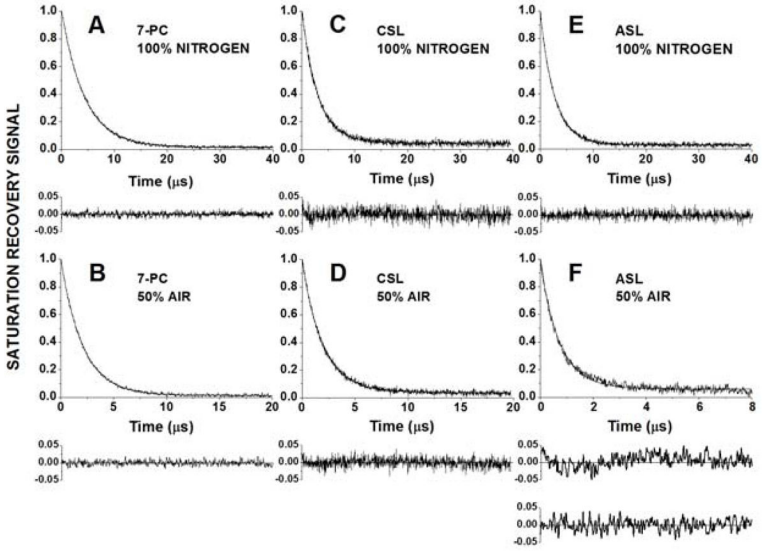

Fig. 5.

Representative saturation-recovery signals with fitted curves and the residuals (the experimental signal minus the fitted curve) for 7-PC (A,B), CSL (C,D), and ASL (E,F) in the membranes made of lens lipids isolated from the nuclear fraction of fiber cells of cow eyes. Signals were recorded at 25°C for samples equilibrated with 100% nitrogen gas (A,C,E) and with gas mixture of 50% air and 50% nitrogen (B,D,F). Saturation-recovery signals for 7-PC and CSL were satisfactorily fitted to a single exponential function in both the absence and presence of molecular oxygen with time constants 4.37 ± 0.01 μs (A), 2.05 ± 0.01 μs (B), 2.95 ± 0.01 μs (C), and 1.91 ± 0.01 μs (D). For ASL the saturation-recovery signal in the presence of molecular oxygen can be fit satisfactorily only with double exponential curve with time constants 1.50 ± 0.28 μs and 0.55 ± 0.04 μs (compare the upper residual for single and lower residual for double exponential fit in F), whereas single-exponential fit with time constant 2.71 ± 0.01 μs was satisfactory in the absence of molecular oxygen (E). Additional criteria for the goodness of a single and double-exponential fits are explained in Note 16.

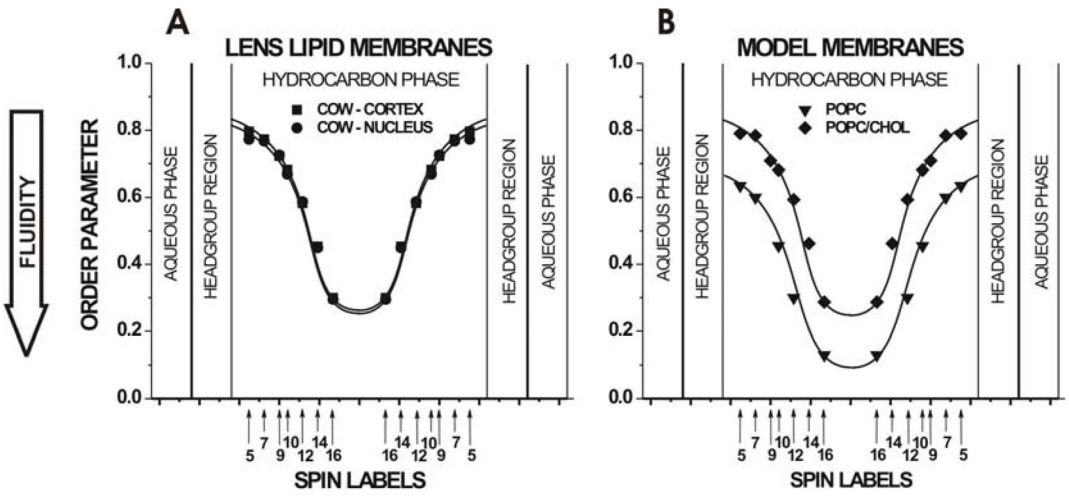

Fig. 6.

Profiles of the molecular order parameter at 25°C obtained with n-PC and n-SASL across membranes made of cortical and nuclear cow lens lipids are presented in (A) and across membranes made of POPC/Chol equimolar mixture and of pure POPC are presented in (B). Approximate localizations of nitroxide moieties of spin labels are indicated by arrows. For POPC and POPC/Chol membranes data were taken from Refs. 9 and 11.

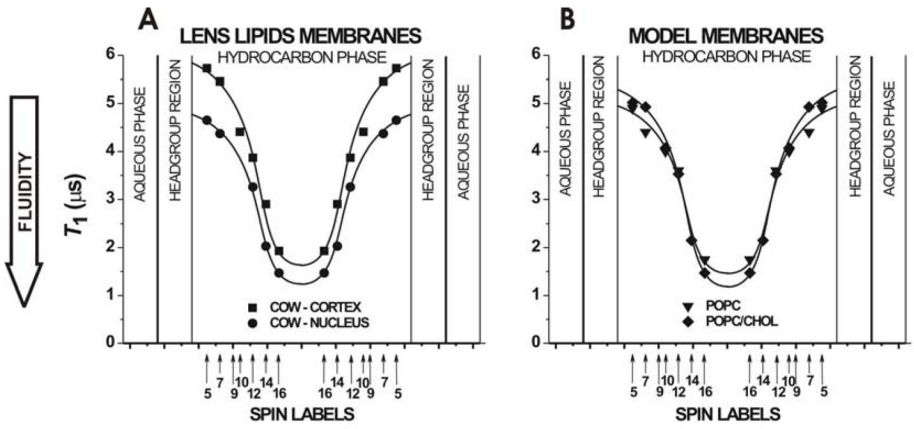

Fig. 7.

Profiles of the electron spin-lattice relaxation time, T_1, for n-PC spin labels at 25°C across membranes made of cortical and nuclear cow lens lipids are presented in (A) and across membranes made of POPC/Chol equimolar mixture and of pure POPC are presented in (B). Approximate localizations of nitroxide moieties of spin labels are indicated by arrows. For POPC membranes data were taken from Ref. 40.

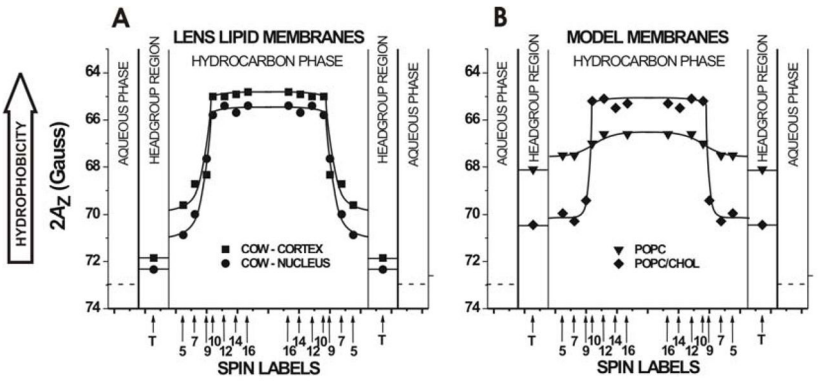

Fig. 8.

Hydrophobicity profiles ($2A_Z$) across membranes made of cortical and nuclear cow lens lipids are presented in (A) and across membranes made of POPC/Chol equimolar mixture and of pure POPC are presented in (B). Upward changes indicate increases in hydrophobicity. Because T-PC contains a different nitroxide moiety than n-PC and n-SASL, its points are not connected with other points. However, the relative changes of the hydrophobicity in the polar headgroup region can be evaluated (*see* Note 13). Broken lines indicate hydrophobicity in the aqueous phase (*see* Note 13). Approximate localizations of nitroxide moieties of spin labels are indicated by arrows. For POPC and POPC/Chol membranes data were taken from Refs. 9 and 11.

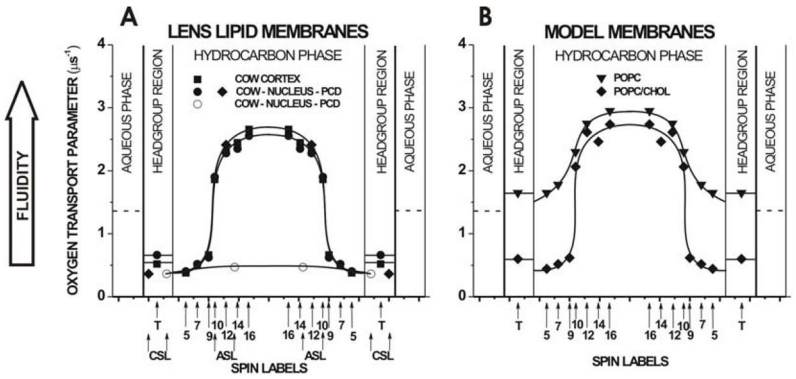

Fig. 9.

Profiles of the oxygen transport parameter (oxygen diffusion-concentration product) at 25°C across membranes made of cortical and nuclear cow lens lipids are presented in (A) and across membranes made of POPC/Chol equimolar mixture and of pure POPC are presented in (B). Broken lines indicate the oxygen transport parameter in the aqueous phase. Approximate localizations of nitroxide moieties of spin labels are indicated by arrows. For POPC and POPC/Chol membranes data were taken from Refs. 9 and 40.